MOLECULAR AND CELLULAR BIOLOGY, May 1991, p. 2675–2685
0270-7306/91/052675-11$02.00/0

Vol. 11, No. 5

Cell Surface Transport, Oligomerization, and Endocytosis of Chimeric Type II Glycoproteins: Role of Cytoplasmic and Anchor Domains

AMITABHA KUNDU, M. ABDUL JABBAR† AND DEBI P. NAYAK*

Jonsson Comprehensive Cancer Center and Department of Microbiology and Immunology, University of California at Los Angeles School of Medicine, Los Angeles, California 90024-1747

Received 17 December 1990/Accepted 1 March 1991

We investigated the role of cytoplasmic and anchor domains of type II glycoproteins in intracellular transport, oligomerization, and endocytosis by expressing the wild-type and chimeric genes in mammalian cells. Chimeric genes were constructed by exchanging the DNA segments that encode the cytoplasmic and anchor domains between the human influenza virus (A/WSN/33) neuraminidase (NA) and transferrin receptor (TR). The chimeric proteins in which domains were exchanged precisely were productively targeted to the cell surface. However, the proteins appeared to assemble differently in the intracellular compartment. For example, while TR existed predominantly as a dimer, NATRΔ90, containing the cytoplasmic and signal-anchor domains of NA and the ectodomain of TR, was present as a tetramer, a dimer, and a monomer. Similarly, the influenza virus NA existed predominantly as a tetramer but TRNAΔ35, in which the cytoplasmic and signal-anchor domains of TR were joined to the ectodomain of NA, existed predominantly as a dimer, suggesting that the cytoplasmic and anchor domains of type II glycoproteins affect the subunit assembly of heterologous ectodomains. In addition, we analyzed the role of the cytoplasmic domain in endocytosis. NA and NATRΔ90 did not undergo endocytosis, whereas both TR and TRNAΔ35 were internalized efficiently, demonstrating that the NH_2 cytoplasmic domain of TR was capable of internalizing a heterologous ectodomain (NA) from the cell surface.

The integral membrane glycoproteins of enveloped viruses play a major role in tissue tropism, as well as in viral pathogenesis. Of the three transmembrane proteins present on the influenza viral envelope, the hemagglutinin and neuraminidase (NA) have been well characterized (7, 8, 54, 56). Hemagglutinin, a type I membrane glycoprotein, is the major surface glycoprotein involved in viral receptor binding and infection (see reference 41). NA, on the other hand, possesses receptor-destroying activity and is primarily responsible for elution and spread of the virus (44). It is a type II glycoprotein possessing an uncleaved signal-anchor domain and is anchored in the membrane at its amino terminus (3, 41). The atomic structure of NA has been elucidated, and major antigenic sites have been mapped (7, 54). NA is a homotetramer, and the extracellular globular domain possesses the glycosylation sites, antigenic epitopes, and the enzyme active site (8, 41, 54).

Workers in our laboratory have been interested in elucidating the functions of different domains of membrane glycoproteins in translocation, as well as in intracellular transport and sorting (12, 23, 37–39). Our earlier studies with influenza virus hemagglutinin and vesicular stomatitis virus G, type I membrane glycoproteins, have shown that when the NH_2 signal domain or the COOH anchor and cytoplasmic domains were precisely switched between these glycoproteins, the chimeric proteins were transported to the cell surface and exhibited functions of the corresponding ectodomain (38, 39). On the other hand, fusion within the ectodomain resulted in generation of chimeric proteins that were defective in intracellular and cell surface transport (37).

In recent years, we have carried out experiments to understand the functions of discrete domains of NA, a type II membrane protein which contains three spatially separated domains: the NH_2-terminal cytoplasmic domain, a hydrophobic domain, and an ectodomain (the stalk and globular head). The hydrophobic domain has been shown to function both as a signal sequence for translocation of the protein across the endoplasmic reticulum (ER) and as a transmembrane sequence for anchoring of the protein in the membrane (3). Mutational analyses of the transmembrane domain have shown the importance of certain critical amino acid residues in translocation, as well as intracellular transport (53). Furthermore, deletion mutations in the hydrophobic region demonstrated the absence of specific subdomains that might function either solely as the ER translocation signal or transmembrane anchor domain (6, 41). However, the contributions of different domains, particularly, the transmembrane and cytoplasmic domains in intracellular transport and oligomerization of a type II membrane protein, have not been systematically assessed.

In the present study, we carried out gene fusion between two type II membrane glycoproteins, human influenza virus NA and transferrin receptor (TR). The cytoplasmic and signal-anchor domains of NA and TR were exchanged to generate chimeric type II glycoproteins. Our data show that these chimeric proteins were transported to the cell surface like their wild-type (WT) counterparts and that the anchor and cytoplasmic domains play a critical role in subunit assembly of the ectodomains to which they are tethered. Furthermore, the anchor and cytoplasmic domains of TR, which possess the information for internalization, also functioned in the endocytosis of a heterologous ectodomain (NA).

* Corresponding author.
† Present address: Department of Molecular Biology, Research Institute, The Cleveland Clinic Foundation, Cleveland, OH 44195.

MATERIALS AND METHODS

Cells, viruses, plasmids, and antibodies. CV-1 cells were grown in Dulbecco modified Eagle medium supplemented with 10% fetal bovine serum. Vaccinia virus stocks were prepared in HeLa cells as reported previously (35). The vaccinia virus containing the T7 polymerase gene was kindly provided by Bernard Moss, National Institutes of Health, Bethesda, Md. (15). The plasmid containing the human TR cDNA (29) was a gift from F. Ruddle, Yale University, New Haven, Conn. Anti-TR monoclonal antibody was obtained from Amersham, Arlington Heights, Ill. Fluorescein isothiocyanate-conjugated goat anti-rabbit and goat anti-mouse immunoglobulins were bought from Caltag, South San Francisco, Calif. Polyclonal antibodies against the WSN influenza virus and WSN NA peptides were raised in rabbits. Anti-NA monoclonal antibodies were kindly provided by Walter Gerhard, Wistar Institute, Philadelphia, Pa., and Peter Palese, Mt. Sinai Medical Center, New York, N.Y. Lipofectin was purchased from Bethesda Research Laboratories, Gaithersburg, Md., and used in transfection assays.

Plasmid construction. TRNAΔ26. To construct pGTRNA Δ26, pGTR (29) was digested with *Dde*I and the 360-bp fragment containing the signal-anchor domain of TR was filled in with DNA polymerase I (Klenow fragment) to produce a blunt end. This fragment was cloned into pGem-3, which had been digested with *Hin*cII, and filled in with DNA polymerase I (Klenow fragment) to generate plasmid pGTRAS, containing the signal-anchor domain of TR. pGNAΔ26 (12) was digested with *Eco*RI, and the 1,300-bp fragment encoding the ectodomain of NA was filled in with DNA polymerase I (Klenow fragment). This DNA fragment was cloned into pGTRAS, which was digested first with *Pst*I, followed by mung bean nuclease, cut with *Hin*dIII, and then filled in with DNA polymerase I (Klenow fragment) to produce blunt ends. The resulting plasmid in the proper orientation was called pGTRNAΔ26. It contains the cDNA encoding the NH_2 terminus, 97 amino acids of TR (the cytoplasmic and signal-anchor domains of TR), three extraneous amino acids, and the entire ectodomain of NA from residue 27 (Fig. 1A and B).

TRNAΔ35. TRNAΔ35 was obtained by loop-out mutagenesis from plasmid pGTRNAΔ26 by using a 42-mer DNA primer to produce a chimeric cDNA encoding precisely the signal-anchor domain of TR (up to residue 89) and the ectodomain of NA from amino acid 36 (20).

NATRΔ152. To construct NATRΔ152, pGTR was digested with *Nde*I, followed by mung bean nuclease to produce a blunt end, and then *Sal*I to generate a 1,900-bp DNA fragment encoding the entire 671-amino-acid external domain of TR. This DNA fragment was cloned into pGN40 (3), possessing the cDNA for the first 40 amino acids of NA. pGN40 was digested with *Bam*HI, filled in with the Klenow fragment of DNA polymerase I to produce a blunt end, and finally digested with *Sal*I. The resulting plasmid, pGNATRΔ152, encodes a chimeric protein which possesses the cytoplasmic and signal-anchor domains of NA up to residue 40 of NA, three extraneous amino acids, and the ectodomain of TR from residue 153 of TR.

NATRΔ90. A DNA segment (1,100 bp) containing the 5′ portion of the NA cDNA was isolated by *Eco*RI and *Bam*HI digestion of pGNA (3). The DNA segment was cloned into M13mp18, and an *Eco*RI site was created at bp 129 of the NA fragment by in vitro mutagenesis. The 129-bp NA DNA segment was isolated by *Eco*RI digestion. Similarly, an *Eco*RI site was created at bp 361 of the TR fragment in M13mp18 by in vitro mutagenesis. The fragment (361 bp) containing *Eco*RI and *Hin*dIII sites was isolated and used for three-way ligation with the 129-bp NA DNA segment and the pGTR DNA segment (*Eco*RI to *Hin*dIII) to obtain pGNATRΔ90. The resulting plasmid contains the cDNA encoding the cytoplasmic and signal-anchor domains of NA (up to residue 35) and the entire ectodomain of TR from residue 90. All chimeric DNA constructs were sequenced through the junction site to determine the nucleotide and predicted amino acid sequences at the fusion point (Fig. 1A and B).

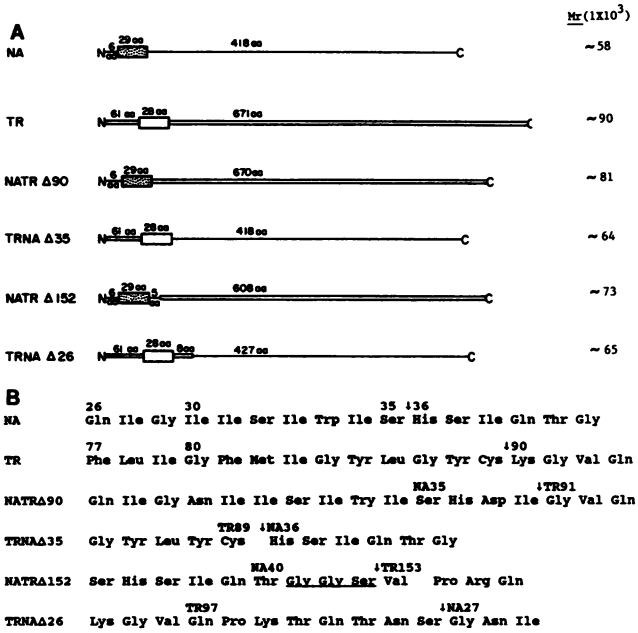

FIG. 1. Schematic representation and amino acid (aa) sequences at the junction of influenza virus NA and human TR chimeras. (A) Dotted boxes and single lines represent the influenza virus NA sequence, and open boxes and double lines represent the human TR sequence. (B) Vertical arrows show the junction of the hydrophobic anchor domain and ectodomain in NA (amino acid 35), TR (amino acid 89), TRNAΔ35, and NATRΔ90. The extraneous amino acids acquired during construction from linkers are underlined.

Transfection, indirect immunofluorescence, radiolabeling, immunoprecipitation, and endo H treatment. Essentially, the procedure of Fuerst et al. (15) for transient expression was followed. Briefly, CV-1 cells were infected with vaccinia virus expressing T7 RNA polymerase, and the target genes under control of the T7 promoter were introduced to the virus-infected cells by lipofectin-mediated gene transfer (14). At 14 to 16 h posttransfection, the cells were fixed and stained for internal (total) and cell surface antigens (24, 40).

For surface staining, cells were fixed with 3.7% formaldehyde for 10 to 15 min (24), whereas for internal staining cells were fixed and permeabilized with acetone-methanol (1:1) at −20°C (40). Specific antibodies were added to the coverslips containing fixed cells and incubated for 30 min at room temperature. The antibody-treated cells were then washed with phosphate-buffered saline (PBS) and layered with a 1:50 dilution of fluorescein isothiocyanate-conjugated antiantibody for 30 min at room temperature and examined with a Nikon photomicroscope by epifluorescence (24, 40).

For pulse-chase experiments, the transfected cells at 16 h posttransfection were pulse-labeled for 15 min with 100 μCi

each of [^{35}S]methionine (ICN, Irvine, Calif.) and [^{35}S]cysteine (Amersham) per ml. At the end of the pulse, unlabeled cysteine and methionine were added to 20 mM and chased for different times. Approximately 5×10^5 cells (60-mm-diameter dish) were lysed in 0.5 ml of RIPA buffer (50 mM Tris HCl [pH 7.6], 150 mM NaCl, 0.5% Triton X-100, 0.5% deoxycholate, 0.1% sodium dodecyl sulfate [SDS], 1 mM phenylmethylsulfonyl fluoride). For immunoprecipitation, the lysates (0.5 ml) were incubated with either monoclonal (anti-TR) or polyclonal (anti-NA made against NA peptides or WSN virus) antibodies (5 μl) for 2 h on ice, protein A-Sepharose (5 mg) was added, and the mixture was shaken for 2 to 3 h. The beads containing the immune complexes were collected and washed three times with RIPA buffer containing 5 mg of bovine serum albumin and 0.5 M NaCl and finally again with RIPA buffer (23, 24). The immunoprecipitated protein samples were dissolved by boiling in 40 μl of sample buffer (6.5 mM Tris HCl [pH 6.8], 10% glycerol, 2% SDS, 5% β-mercaptoethanol) and electrophoresed on SDS–10% polyacrylamide gels (30).

For endo-β-*N*-acetylglucosaminidase H (endo H) treatment, the immune complex with the protein A-Sepharose beads was suspended in 20 μl of 1% SDS and heated at 100°C for 3 min. H_2O (180 μl) was added, and the sample was boiled again for 1 min. The beads were removed, and the supernatant was adjusted to 50 mM sodium acetate, pH 5.5. One half of the sample was treated with 10 mU of endo H for 16 h at 37°C, and the other half was mock treated (24).

Quantitation of viral membrane proteins at the cell surface. Transfected cells were pulse-labeled and chased for different times. For surface labeling, the cells were washed with cold PBS and treated with 0.5 mg of Sulfo-NHS-Biotin (Pierce Chemical Co., Rockford, Ill.) for 30 min at 4°C. The cells were then washed four times with PBS, lysed, and immunoprecipitated (32, 34, 51). The immunoprecipitate was eluted by being boiled twice in 100 μl of elution buffer (1% SDS, 0.2 M Tris HCl [pH 8.8], 5 mM ethylene glycol-bis(β-aminoethyl ether)-*N*,*N*,*N*′,*N*′-tetraacetic acid) for 2 min and then washed with 300 μl of RIPA buffer. Eluates and the wash were pooled and incubated with 50 μl of a 50% slurry of streptavidin-agarose beads (Pierce) for 30 min at 4°C. The beads were then washed three times as described above and boiled in sample buffer, and the supernatant was analyzed by SDS-polyacrylamide gel electrophoresis (30).

Parallel cultures were treated with proteinase K in PBS for 60 min at 4°C to remove membrane proteins at the cell surface (34). Further digestion was stopped by addition of phenylmethylsulfonyl fluoride (Calbiochem, San Diego, Calif.) to a final concentration of 0.2 mg/ml for 20 min on ice. The proteinase K-treated and untreated cells were lysed with RIPA buffer and immunoprecipitated as described above.

Sucrose velocity gradient centrifugation. For velocity gradient sedimentation, the transfected cells were labeled with [^{35}S]methionine (100 μCi/ml) and [^{35}S]cysteine (100 μCi/ml) for 30 min, followed by a chase of 90 min, and lysed in 0.5 ml of MNT buffer (20 mM morpholineethanesulfonic acid, 100 mM NaCl, 30 mM Tris HCl [pH 7.6], 0.5% Triton X-100). Cells from eight dishes (60-mm diameter) were lysed, and nuclei and other insoluble components were removed by centrifugation in a microcentrifuge for 10 min. The lysate was layered on top of a 12-ml 5 to 20% sucrose gradient in MNT buffer and centrifuged for 20 h at 4°C in a Beckman SW40 rotor at 40,000 rpm (10). Fractions were collected from the bottom of the gradient, and each fraction was precipitated with specific antibodies and analyzed by SDS-polyacrylamide gel electrophoresis. Catalase (240 kDa; 11.3S), influenza virus hemagglutinin trimer (210 kDa; 10S), and aldolase (160 kDa; 8.6S) were used as markers in parallel gradients. Sedimentation values of the proteins in the gradient were measured as previously described (36).

Antibody uptake assay. Antibody uptake experiments were carried out essentially as previously described (31). Briefly, transfectants (grown on cover glass in 35-mm-diameter dishes) expressing the WT and chimeric proteins were shifted down to 4°C for 1 h. The cells were then washed four or five times in ice-cold PBS and incubated with specific mouse monoclonal antibodies (1:50 dilutions in 1 ml of Dulbecco modified Eagle medium buffered with 10 mM HEPES [*N*-2-hydroxyethylpiperazine-*N*′-2-ethanesulfonic acid]) at 4°C for 1 h. Unbound antibodies were removed by washing the cells five times in ice-cold PBS and shifted up to 37°C in a CO_2 incubator in Dulbecco modified Eagle medium. At the times indicated, the dishes were shifted down to 4°C for 1 h. One set of dishes was kept at 4°C throughout the experiment. At the end of the experiment, the cells were washed, fixed in acetone-methanol (1:1), and stained for specific antibodies by using fluorescein isothiocyanate-conjugated sheep anti-mouse antibodies.

Antigen localization in intracellular vesicles. Transfectants expressing the WT and chimeric proteins were treated with cycloheximide (100 μg/ml) at 37°C for 3 h to block further protein synthesis and to chase the previously synthesized proteins to the plasma membrane. At the end of the chase period, 50 mM chloroquine was added to the cells for another 3 h at 37°C. Cycloheximide was present throughout the experiment. Cells were then washed in PBS, fixed with acetone-methanol (1:1), and stained for the specific antigens as described above.

RESULTS

Cellular localization of WT and chimeric proteins. cDNA constructs that encode the WT and chimeric proteins were introduced by lipofectin-mediated DNA transfer into CV-1 cells which were infected with vaccinia viruses expressing T7 RNA polymerase (15). At 15 to 20 h posttransfection, the cells were fixed and examined for expression of proteins by indirect immunofluorescence assay as described in Materials and Methods. Figure 2 presents the intracellular (total) and cell surface expression of proteins in CV-1 cells. WT NA and TR, as well as the chimeras NATRΔ90 and TRNAΔ35, were productively targeted to the cell surface (Fig. 2A, E, G, and K). However, chimeric proteins TRNAΔ26 and NATRΔ152, which contained additional sequences of the ectodomains, failed to be expressed at the cell surface (Fig. 2C and I) and were present intracellularly in the perinuclear region (Fig. 2D and J), suggesting that these chimeras were blocked in the ER or *cis* Golgi region of the cell. These results demonstrated that the productive cell surface delivery of chimeric type II glycoproteins required precise exchange of domains, as has been shown for type I proteins (9, 37–39, 48, 50).

Intracellular transport and processing of WT and chimeric NAs. The processing kinetics of the WT and chimeric proteins were examined by pulse-chase experiments as described in Materials and Methods. After 15 min of pulse-labeling, the WT NA exhibited two glycosylated forms approximately in equal amounts (Fig. 3A). Molecular weight estimates suggest that these two forms possess three and four carbohydrate chains. During the chase, however, the higher-molecular-weight form became predominant but a fraction of the protein existed in the lower-molecular-weight form, even after a 5-h chase. After a 1-h chase, both forms of

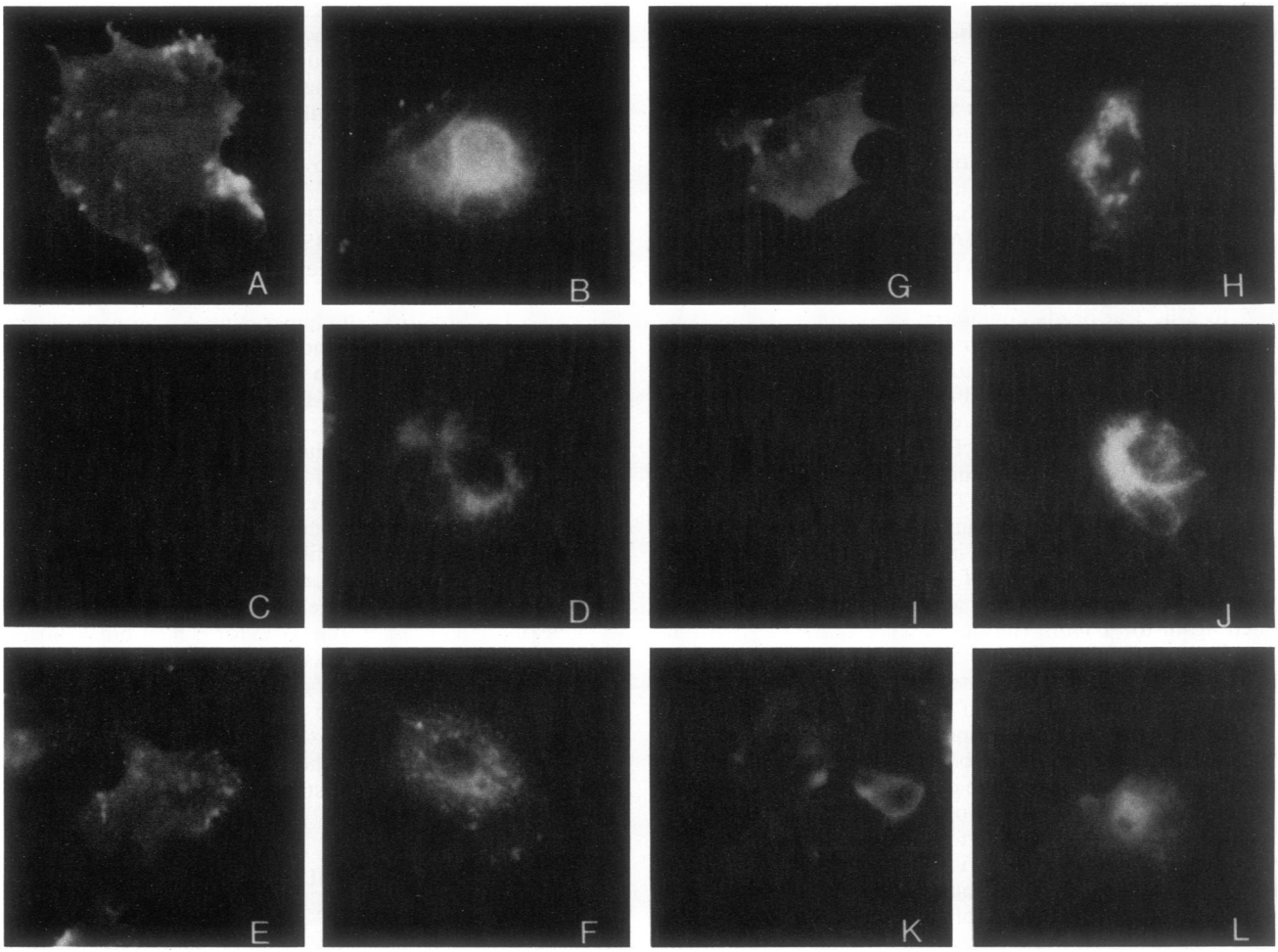

FIG. 2. Cell surface and intracellular (total) immunofluorescence of NA, TR, and chimeric proteins. CV-1 cells were infected with vaccinia virus and transfected with WT or chimeric cDNA and stained for the cell surface and protein by indirect intracellular (total) immunofluorescence. Fluorescence: Panel A, NA at the cell surface; panel B, intracellular; panel C, TRNAΔ26 at the cell surface; panel D, intracellular; panel E, TRNAΔ35 at the cell surface; panel F, intracellular; panel G, TR at the cell surface; panel H, intracellular; panel I, NATRΔ152 at the cell surface; panel J, intracellular; panel K, NATRΔ90 at the cell surface; panel L, intracellular.

WT NA appeared to be completely sensitive to endo H, and only after a longer chase did a very small fraction (less than 10%) exhibit partial resistance to endo H (Fig. 3A, arrowheads on the right). These data suggest that although four glycosylation sites of WT NA were modified by addition of core oligosaccharide chains, only one or two sites acquired endo H resistance in a small fraction of NA. Similar heterogeneity in the glycosylation and endo H resistance of NA was observed in WSN virus-infected CV-1 cells (Fig. 3E), as well as in transfected CV-1 cells at 6 h posttransfection (data not shown). TRNAΔ35 showed subtle differences in the glycosylation pattern compared with WT NA. Protein molecules containing two, three, or four oligosaccharides were present in nearly equal amounts during the pulse-labeling and chase, except at 5 h, when two rather than three forms were present (Fig. 3B). Furthermore, unlike WT NA, TRNAΔ35 acquired partial endo H resistance earlier (e.g., within 1 h of the chase) and in a larger fraction of the protein (Fig. 3B). Although some heterogeneity was observed among the endo H-resistant forms, one species became predominant during the chase. TRNAΔ26 acquired only endo H-sensitive modifications (data not shown), supporting the indirect immunofluorescence finding (Fig. 2D) that the protein was blocked in the ER or *cis* Golgi (26, 47).

Since oligosaccharide processing and Endo H resistance of WT and chimeric NAs could not be used quantitatively to determine the rate of cell surface transport of the proteins, we used a biotinylation procedure to assay the cell surface proteins (32, 51). Parallel cultures were also used to determine the total and internal amounts of labeled proteins after removal of cell surface proteins by protease K treatment (Fig. 4). At different chase times, cell surface, total, or internal proteins were recovered by immunoprecipitation. However, since the biotin-streptavidin assay appears to recover only a fraction of the surface protein (references 32 and 34; Fig. 4) this procedure does not measure the precise amount of the protein on the cell surface. Therefore, the precise efficiency of cell surface transport of NA or TRNAΔ35 could not be determined. However, relative values with or without protease treatment provided an estimate of the cell surface transport of individual proteins (Fig. 4B) and suggested that approximately 70% of NA and 30% of TRNAΔ35 reached the cell surface by 4 h of the chase. However, the estimate for chimeric TRNAΔ35 may

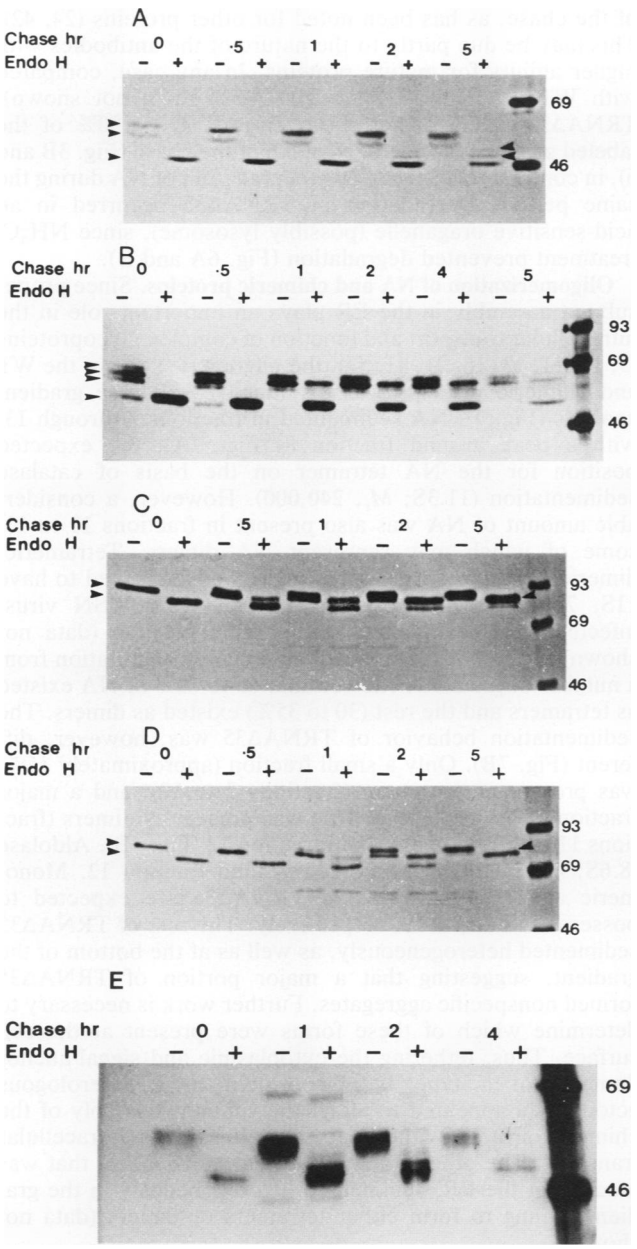

FIG. 3. Analysis of NA, TRNAΔ35, TR, and NATRΔ90 polypeptides for glycosylation. Transfected cells were labeled with [^{35}S]methionine and [^{35}S]cysteine for 15 min (0) at 16 h posttransfection and chased for the time periods shown (in hours) at the top of each panel. Panels: A, NA; B, TRNAΔ35; C, TR; D, NATRΔ90; E, NA in WSN virus-infected cells. Immunoprecipitated samples were either treated with endo H (+) or untreated (−). Marker protein sizes are shown in kilodaltons.

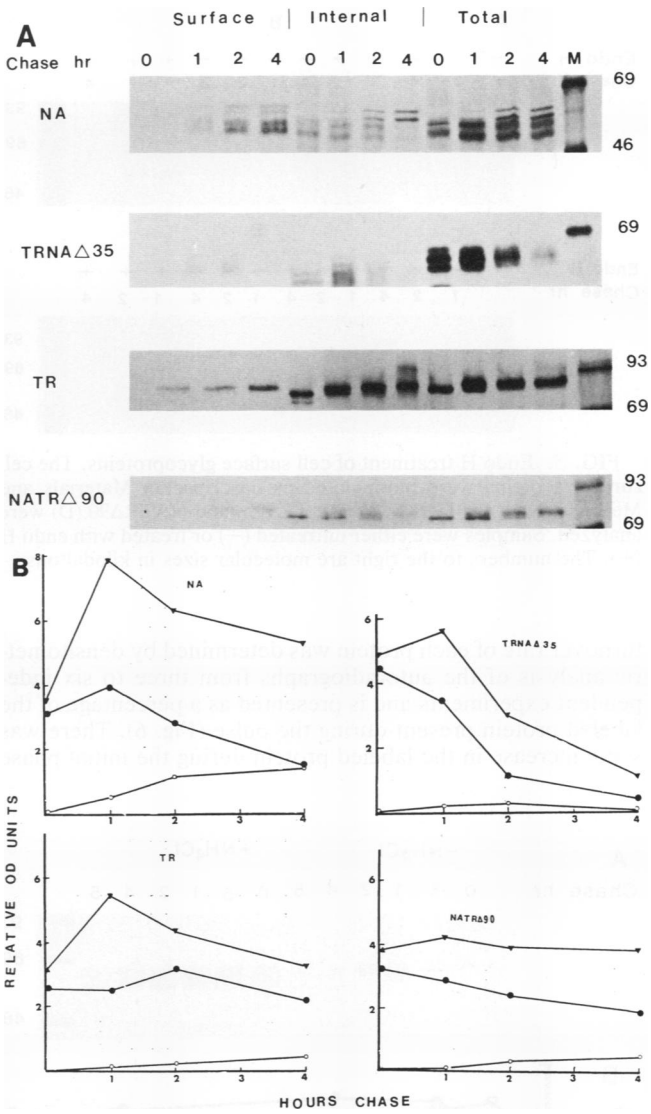

FIG. 4. Expression of WT and chimeric proteins on the surface of cells. CV-1 cells were transfected with NA, TRNAΔ35, TR, and NATRΔ90 DNAs, pulsed for 15 min with [^{35}S]cysteine and [^{35}S]methionine, and chased for 0, 1, 2, and 4 h. The cell surface proteins were biotinylated as described in Materials and Methods. Parallel cultures with or without protease treatment were analyzed for total and internal proteins. Samples were analyzed by SDS-polyacrylamide gel electrophoresis and processed for autoradiography (A), and bands were quantified by densitometry (B). Symbols: ▼, total membrane protein; ●, internal protein left after proteinase K treatment; ○, biotinylated proteins. One-third of the total and proteinase K-treated samples and all of the biotinylated samples were used for gel analysis. For quantification, values were normalized. The numbers to the right of the gel are molecular sizes in kilodaltons.

be less precise because of its cell surface instability (Fig. 4A) and intracellular degradation (see Fig. 6B). Biotinylation data indicated that WT NA and TRNAΔ35 were transported to the cell surface with a half-life of approximately 1 to 1.5 h.

To determine the nature of the oligosacchaarides present on the cell surface proteins, the biotinylated proteins were treated with endo H. Both endo H-sensitive and partially endo-H resistant forms of NA and TRNAΔ35 (Fig. 5A and B) were present on the cell surface, suggesting that acquisition of endo H resistance was not a prerequisite for acquisition of cell surface transport competence, as has also been reported for other membrane-anchored proteins (18, 19). Heterogeneity in endo H resistance has been observed for NA in WSN virus-infected CV-1 cells (Fig. 3E) and hemagglutinin-NA in simian virus 5-infected cells (42), as well as for Thy-1 protein (49).

Intracellular stability of WT and chimeric proteins. The

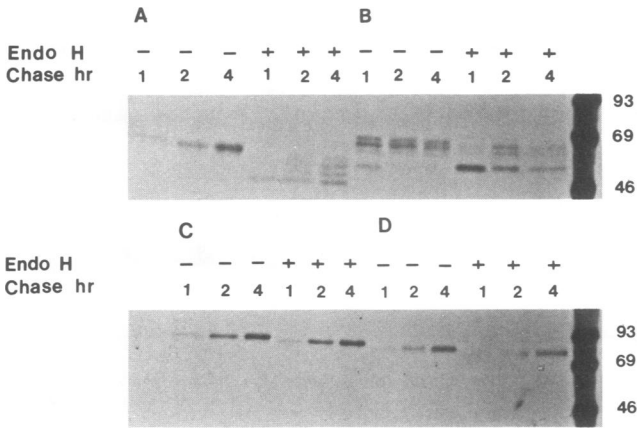

FIG. 5. Endo H treatment of cell surface glycoproteins. The cell surface proteins were biotinylated as described in Materials and Methods. NA (A), TRNAΔ35 (B), TR (C), and NATRΔ90 (D) were analyzed. Samples were either untreated (−) or treated with endo H (+). The numbers to the right are molecular sizes in kilodaltons.

turnover rate of each protein was determined by densitometric analysis of the autoradiographs from three to six independent experiments and is presented as a percentage of the labeled protein present during the pulse (Fig. 6). There was some increase in the labeled protein during the initial phase of the chase, as has been noted for other proteins (24, 42). This may be due partly to the nature of the antibodies with higher affinity for mature proteins. In any case, compared with WT NA (Fig. 3A) or TRNAΔ26 (data not shown), TRNAΔ35 had a higher turnover rate. Over 50% of the labeled protein was degraded at 5 h of the chase (Fig. 3B and 6), in contrast to less than 20% degradation of NA during the same period. Degradation of TRNAΔ35 occurred in an acid-sensitive oraganelle (possibly lysosome), since NH_4Cl treatment prevented degradation (Fig. 6A and B).

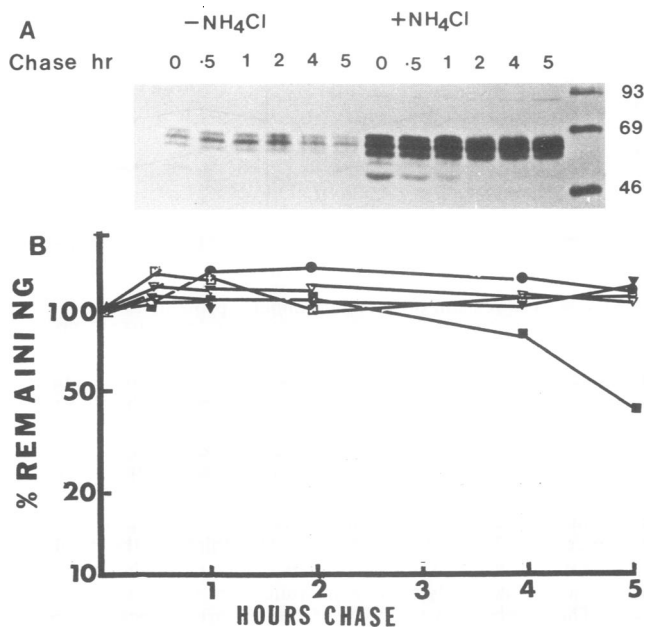

FIG. 6. Inhibition of degradation of TRNAΔ35 by NH_4Cl. (A) Transfected cells were labeled with [^{35}S]methionine and [^{35}S]cysteine for 10 min (0) and chased in the presence (+) or absence (−) of NH_4Cl for the different periods shown at the top (in hours). NH_4Cl (30 mM) was present during the pulse-labeling and chase periods. (B) Amounts of NA (●), TR (□), NATRΔ90 (▼), and TRNAΔ35 in the presence (▽) or absence (■) of NH_4Cl were quantified by densitometric tracing of autoradiographs. An average of three to six independent experiments was used for each protein. The data are presented as percentages of the protein present during the pulse-labeling period. The numbers to the right of the gel are molecular sizes in kilodaltons.

Oligomerization of NA and chimeric proteins. Since proper subunit assembly in the ER plays an important role in the intracellular transport and function of complex glycoproteins (5, 10, 11, 13, 16, 21, 41, 57), the oligomeric state of the WT and chimeric proteins was examined by sucrose gradient analysis (Fig. 7). NA sedimented in fractions 7 through 13, with a peak around fraction 8 (Fig. 7A), the expected position for the NA tetramer on the basis of catalase sedimentation (11.3S; M_r, 240,000). However, a considerable amount of NA was also present in fractions 11 to 13, some of which may represent NA dimers. Tetrameric, dimeric, and monomeric forms of NA are expected to have 11S, 7S, and 4.4S, respectively. NA from WSN virus-infected cells sedimented in the same position (data not shown) as the NA from transfected cells. Quantitation from a number of gradients showed that 65 to 70% of NA existed as tetramers and the rest (30 to 35%) existed as dimers. The sedimentation behavior of TRNAΔ35 was, however, different (Fig. 7B). Only a small fraction (approximately 15%) was present as tetramers (fractions 7 to 10), and a major fraction of the protein (≈40%) was present as dimers (fractions 11 to 13), with a peak in fraction 12 (Fig. 7B). Aldolase (8.6S; M_r 160,000) sedimented around fraction 12. Monomeric and dimeric forms of TRNAΔ35 are expected to possess 4.7S and 7.4S, respectively. The rest of TRNAΔ35 sedimented heterogeneously, as well as at the bottom of the gradient, suggesting that a major portion of TRNAΔ35 formed nonspecific aggregates. Further work is necessary to determine which of these forms were present at the cell surface. Thus, tethering the cytoplasmic and signal-anchor domains of a type II glycoprotein to a heterologous ectodomain appeared to affect the subunit assembly of the chimeric protein without grossly altering its intracellular transport. The other chimeric protein, TRNAΔ26, that was blocked in the ER, sedimented heterogeneously in the gradient, failing to form either tetramers or dimers (data not shown).

Enzymatic activities of WT and chimeric NAs. The enzymatic activities of the WT and chimeric NAs in transfected cells were examined and compared with the activities in WSN virus-infected cells. Lysates of CV-1 cells infected (1/16 of a 60-mm-diameter dish) with WSN (multiplicity of infection, 3) or transfected with recombinant DNA were prepared 16 h posttransfection and assayed for NA activity with fetuin (2, 4). Samples contained identical amounts of protein. Dot blot analysis with polyclonal NA-specific antibodies (4) showed that the relative expression levels of NA, TRNAΔ35, and TRNAΔ26 per microgram of total protein in transfected cells were essentially the same but one-third of that in WSN virus-infected cells. The A_{549}s of WSN-infected and NA-, TRNAΔ35, and TRNAΔ26-transfected cells were 1.54, 0.59, 0.12, and 0.05, respectively. However, since only 5 to 10% of the cells were transfected with NA cDNA compared with 100% of WSN virus-infected cells, the NA activity per cell would be about three- to fivefold higher in transfected cells than in virus-infected cells. The enzymatic

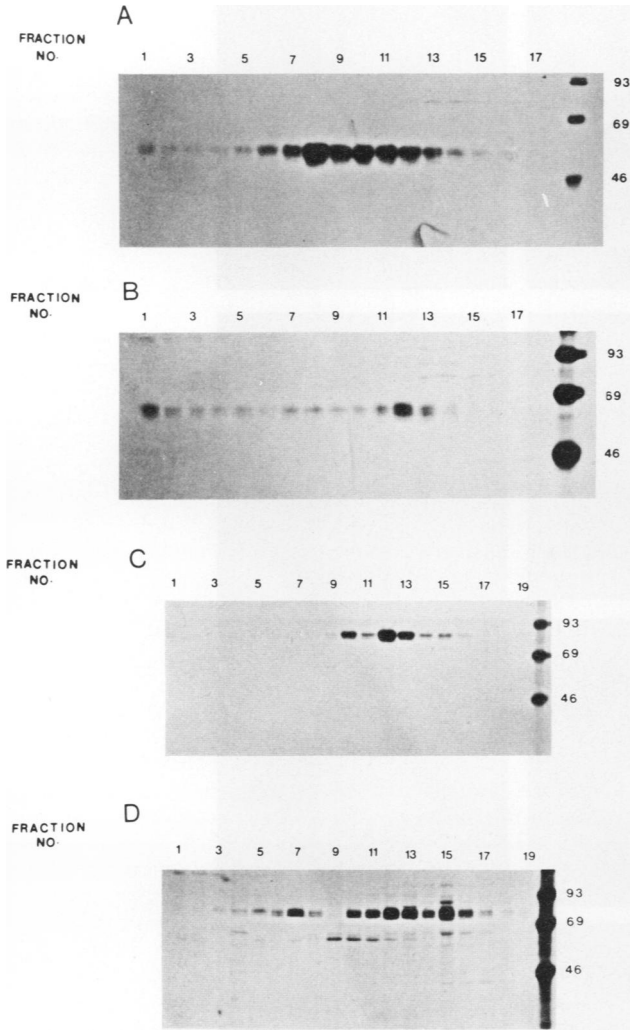

FIG. 7. Sucrose velocity gradient analysis of NA (A), TRNAΔ35 (B), TR (C), and NATRΔ90 (D). Labeled cell lysates were prepared and examined by sucrose velocity gradients as described in Materials and Methods. Fractions were collected and immunoprecipitated with polyclonal antibodies and analyzed by SDS-polyacrylamide gel electrophoresis. Fraction numbers are from the bottom of the tube. Under identical conditions, the marker proteins sedimented as follows: catalase (11.3S; M_r, 240,000), fraction 8; influenza virus hemagglutinin (10S; M_r, 210,000), fraction 10; and aldolase (8.6S; M_r, 160,000), fraction 12. The number on the right are molecular sizes in kilodaltons.

activity of TRNAΔ35-transfected cells was five times less than that of NA-transfected cells. TRNAΔ26-transfected cells exhibited no detectable activity, most likely because of misfolding of the protein in the ER. Since gradient analysis showed that approximately 65 and 15% of NA and TRNAΔ35, respectively, were present as tetramers in transfected cells, our results support the notion that the tetrameric form of NA is the enzymatically active form (8, 45). Furthermore, the labile nature of TRNAΔ35 (Fig. 3B) might also account for the reduced enzymatic acitivity. Direct analysis of fractions from a sucrose or glycerol gradient for the NA activity was unsuccessful, since both sucrose and glycerol were extremely inhibitory for the NA activity assay.

Intracellular transport and processing of TR and chimeric TR proteins. To analyze the kinetics of glycosidic processing, pulse-chase experiments were performed (Fig. 3). The results (Fig. 3C) support the notion that TR had undergone oligosaccharide processing at two glycosylation sites (43, 52). During the chase, however, one of the two oligosaccharide chains acquired endo H resistance (half-life, ≈1 h), as previously observed (52). NATRΔ90 (Fig. 3D) exhibited behavior similar to that of TR (Fig. 3C), except that the kinetics of oligosaccharide processing were somewhat slower compared with those of TR (half-life, 1.5 to 2 h). NATRΔ152, a protein blocked in the ER, was completely endo H sensitive, even at 5 h of the chase (data not shown).

We also examined the kinetics of TR and NATRΔ90 transport to the cell surface by biotinylation and immunoprecipitation (Fig. 4). TR and NATRΔ90 were efficiently transported to the surface with essentially similar kinetics. Approximately 50% of the pulse-labeled protein was transported to the cell surface (Fig. 4). We then examined the nature of the glycosidic modifications of the protein present on the cell surface. Only the partially endo H-resistant forms of both TR and NATRΔ90 were present on the cell surface (Fig. 5C and D).

Sucrose gradient analysis of TR and chimeric TR for oligomerization. The transferrin receptor has been shown to form a disulfide-bonded dimer under nonreducing conditions (1, 43, 52). We therefore wanted to determine the oliogmeric nature of the WT and chimeric TRs expressed from the cDNAs in CV-1 cells. Sucrose gradient fractionation data (Fig. 7C) showed that TR was immunoprecipitated from fractions 10 to 14, with a peak at fraction 12, as expected for a dimeric form of TR (9.3S). These results indicated that the human TR expressed from cDNA behaved like the native protein and was present predominantly as a dimer. However, the chimera NATRΔ90 (monomer 5.5S; M_r, ≈81,000) which was transported to the cell surface exhibited heterogeneous subunit composition (Fig. 7D). The protein sedimented as a monomer (≈40%) (fraction 15), a dimer (≈40%) (fractions 12 and 13), and a tetramer (≈15%) (fraction 7; Fig. 7D). Finally, NATRΔ152, which was blocked in the ER, failed to form specific oligomers and sedimented heteroge-

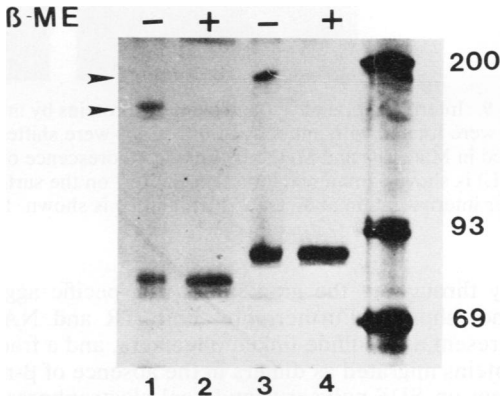

FIG. 8. TR and NATRΔ90 contain disulfide bonds. Transfected cells were labeled with [^{35}S]cysteine and [^{35}S]methionine for 15 min and chased for 2 h. The cells were lysed with RIPA buffer and immunoprecipitated with monoclonal antibody, the samples were treated either without (lanes 1 and 3) or with (lanes 2 and 4) β-mercaptoethanol (β-ME) and analyzed by SDS-polyacrylamide gel electrophoresis. Lanes: 1 and 2, NATRΔ90; 3 and 4, TR. The numbers on the right are molecular sizes in kilodaltons. The arrowheads indicate disulfide-linked oligomers.

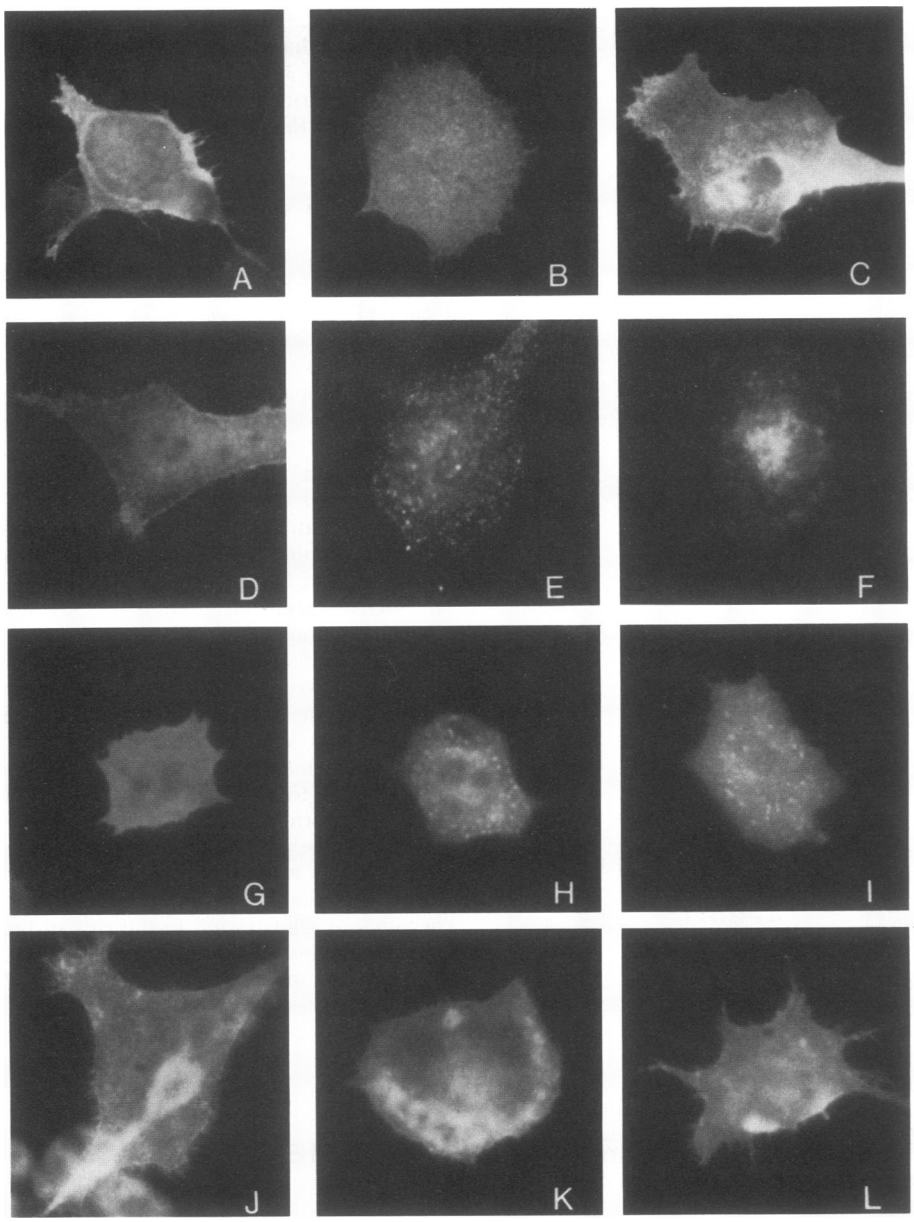

FIG. 9. Internalization of WT and chimeric proteins by immunofluorescence. Cells expressing NA, TRNAΔ35, TR, and NATRΔ90 at the cell surface were treated with antibody at 0°C. Cells were shifted to 37°C for 15 or 30 min and then processed for indirect immunofluorescence as described in Materials and Methods. Immunofluorescence of NA (A, B, and C) TRNAΔ35 (D, E, and F), TR (G, H, and I), and NATRΔ90 (J, K, and L) is shown. Immunofluorescence at 0°C on the surface (A, D, G, and J), 15 min after internalization at 37°C (B, E, H, and K), and 30 min after internalization at 37°C (C, F, I, and L) is shown. Distinct vesicles are present only in E, F, H, and I and absent in the other panels.

neously throughout the gradient as nonspecific aggregates (data not shown). Furthermore, both TR and NATRΔ90 were present as disulfide-linked oligomers, and a fraction of the proteins migrated as dimers in the absence of β-mercaptoethanol on SDS-polyacrylamide gel electrophoresis (Fig. 8).

Internalization of WT and chimeric TR molecules. To assess the role of the cytoplasmic domain in endocytosis of a heterologous protein, specific antibodies were bound on the surface of cells expressing the WT and chimeric proteins at 4°C and warmed up to 37°C for various times. The cells were then fixed and stained by indirect immunofluorescence for intracellular uptake of an antigen-antibody complex. Cells expressing NA (Fig. 9A to C) or NATRΔ90 (Fig. 9J to L) exhibited diffuse immunofluorescence both at 4°C and throughout incubation at 37°C. On the other hand, TR and TRNAΔ35 also exhibited diffuse immunofluorescence at 4°C (Fig. 9G and D), but upon incubation at 37°C they exhibited punctate vesicular fluorescence, which is characteristic of endosomes (Fig. 9E, F, H, and I). After incubation at 37°C, there was a reduction in the cell surface fluorescence of TRNAΔ35 and most of the antigen-antibody complex appeared to be present in endocytic vesicles (Fig. 9E and F). Cells expressing TR also exhibited intracellular vesicles, indicating that TR-antibody complexes were endocytosed (Fig. 9H and I).

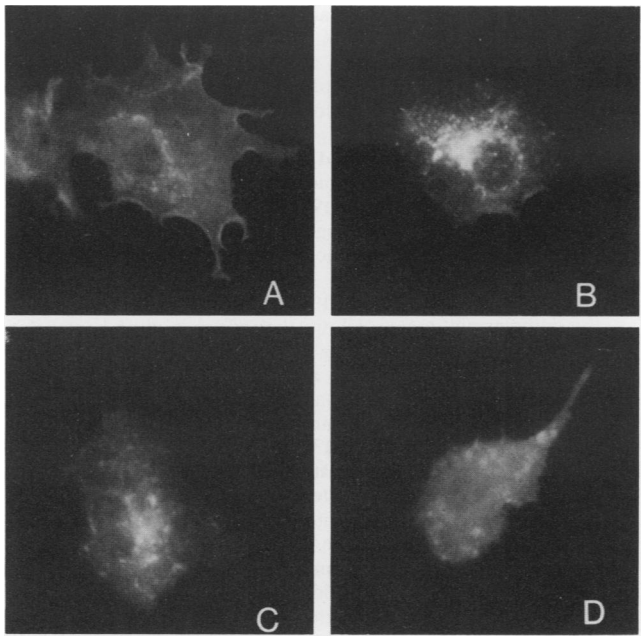

FIG. 10. Antigen localization in intracellular vesicles. Transfected cells were treated with cycloheximide and chloroquine, fixed, and stained as described in Materials and Methods. Panels: A, NA; B, TRNAΔ35; C, TR; D, NATRΔ90. Distinct vesicles are present in panels B and C and absent in A and D.

To determine whether TR and TRNAΔ35 can undergo internalization without antibody binding, the cells expressing specific proteins were incubated with cycloheximide for 3 h and then with cycloheximide and chloroquine for another 3 h. The cells were then stained for internal immunofluorescence with NA- or TR-specific antibodies. Under these conditions, cells expressing NA (Fig. 10A) or NATRΔ90 (Fig. 10D) exhibited diffuse fluorescence, suggesting the presence of the proteins on the cell surface. In contrast, cells expressing TRNAΔ35 (Fig. 10B) or TR (Fig. 10C) exhibited less staining at the cell surface but contained numerous punctate fluorescent vesicles, which are characteristic of endosomes, indicating internalization (28, 31).

DISCUSSION

Transmembrane proteins possess spatially separated distinct domains, such as the ectodomain (head and stalk), the transmembrane domain, and the cytoplasmic tail. Each of these domains is presumed to have a specific role in providing the proper conformation and structural features required for processing, transport, and functional activity. In this study, we exchanged domains between type II membrane proteins (i.e., influenza virus NA and human TR) and generated the chimeric proteins TRNAΔ35 and NATRΔ90, which were transport competent, exhibiting functions of the ectodomain.

Many plasma membrane proteins are present as a homooligomer, a quaternary structure which is critically required not only for their function but also for proper processing and transport through the trafficking pathway (21, 41). Analysis of chimeric proteins NATRΔ90 and TRNAΔ35 suggested that the transmembrane and/or cytoplasmic domain can affect subunit assembly without appreciably interfering with intracellular transport. However, the precise role of the transmembrane and cytoplasmic domains in the assembly process remains to be determined. The transmembrane and cytoplasmic domains may play a critical role in the initial stage of the assembly process by bringing together the subunits, which might become stabilized by interactions of the ectodomains. Alternatively, after assembly of the subunit ectodomains, the oligomer may become stabilized by further interaction among the transmembrane domains (5, 10, 11, 13).

For many proteins undergoing endocytosis, the cytoplasmic domain present in either the NH_2 or COOH terminus appears to be essential for endocytosis (17, 25, 28, 31, 33, 50). Earlier studies using deletion and mutation analyses have shown that the cytoplasmic tail of TR is critical for internalization (22, 25). In the present study, we generated a chimeric protein, TRNAΔ35, that underwent endocytosis in the presence or absence of a bound ligand (e.g., monoclonal antibody) whereas NATRΔ90 failed to undergo endocytosis. These data reinforce the idea that the information for receptor uptake resides predominantly in the cytoplasmic domain of TR. TRNAΔ35 appeared to be degraded in an acid-sensitive membrane compartment, most likely lysosomes. It is possible that some of the proteins could be routed to the lysosomes from the Golgi complex during exocytosis. Alternatively, TRNAΔ35 could be routed to the lysosome after endocytosis. However, recent studies suggest that lysosomal membrane proteins are sorted, probably either at the cell surface or in the *trans* Golgi network, before their delivery to the lysosomes (27, 46, 55). Further work is needed to determine how chimeric protein TRNAΔ35 is routed to and degraded in that compartment.

In summary, our studies have shown that specific domains can be switched precisely between heterologous type II membrane proteins to generate chimeras which are productively transported to the plasma membrane and that analysis of these chimeras can reveal specific functions of the individual domains in intracellular transport, processing, oligomerization, and endocytosis. These chimeras will be valuable in defining the roles of discrete protein domains in the morphogenesis and assembly of virus particles.

ACKNOWLEDGMENTS

The work was partly supported by Public Health Service grants (AI16348, AI12749, and AI25009) to D.P.N. and M.A.J. from the National Institutes of Health.

We thank Cynthia Leon for typing the manuscript.

REFERENCES

1. **Alvarez, E., N. Girones, and R. J. Davis.** 1989. Intermolecular disulfide bonds are not required for expression of the dimeric state and functional activity of the transferrin receptor. EMBO J. 8:2231–2240.
2. **Aminoff, D.** 1961. Methods for quantitative estimation of N-acetyl neuraminic acid and their application to hydrolysates of sialomucoids. Biochem. J. 81:384–392.
3. **Bos, T. J., A. R. Davis, and D. P. Nayak.** 1984. NH_2 terminal hydrophobic region of influenza virus neuraminidase provides the signal function in translocation. Proc. Natl. Acad. Sci. USA 81:2327–2331.
4. **Bos, T. J., and D. P. Nayak.** 1986. Identification of defects in the neuraminidase gene of four temperature-sensitive mutants of A/WSN/33 influenza virus. Virology 154:85–96.
5. **Boulay, F., R. W. Doms, R. G. Webster, and A. Helenius.** 1988. Posttranslational oligomerization and cooperative acid activation of mixed influenza hemagglutinin trimers. J. Cell Biol. 106:629–639.
6. **Brown, D. J., B. G. Hogue, and D. P. Nayak.** 1988. Redundancy of signal and anchor functions in the NH_2-terminal uncharged

region of influenza virus neuraminidase, a class II membrane glycoprotein. J. Virol. **62**:3824–3831.
7. **Colman, P. M., J. N. Varghese, and W. G. Laver.** 1983. Structure of the catalytic and antigenic sites in influenza virus neuraminidase. Nature (London) **303**:41–44.
8. **Colman, P. M., and C. W. Ward.** 1985. Structure and diversity of influenza virus neuraminidase. Curr. Top. Microbiol. Immunol. **114**:178–255.
9. **Compton, T., I. E. Ivanov, T. Gottlieb, M. Rindler, M. Adesnik, and D. Sabatini.** 1989. A sorting signal for the basolateral delivery of the vesicular stomatitis virus (VSV) G protein lies in its luminal domain: analysis of the targeting of VSV G-influenza hemagglutinin chimeras. Proc. Natl. Acad. Sci. USA **86**:4112–4116.
10. **Copeland, C. S., R. W. Doms, E. M. Bolzau, R. G. Webster, and A. Helenius.** 1986. Assembly of influenza hemagglutinin trimers and its role in intracellular transport. J. Cell Biol. **103**:1179–1191.
11. **Copeland, C. S., K. P. Zimmer, K. R. Wagner, G. A. Healey, I. Mellman, and A. Helenius.** 1988. Folding, trimerization, and transport are sequential events in the biogenesis of influenza virus hemagglutinin. Cell **53**:197–209.
12. **Davis, A. R., T. J. Bos, and D. P. Nayak.** 1983. Active influenza virus neuraminidase is expressed in monkey cells from cDNA cloned in simian virus 40 vectors. Proc. Natl. Acad. Sci. USA **80**:3976–3980.
13. **Doms, R. W., A. Runsala, C. Machamer, J. Helenius, A. Helenius, and J. K. Rose.** 1988. Differential effects of mutations in three domains on folding, quaternary structure, and intracellular transport of vesicular stomatitis virus G protein. J. Cell Biol. **107**:89–99.
14. **Felgner, P. L., T. R. Gadek, M. Holm, R. Roman, H. W. Chan, M. Wenz, J. P. Northop, G. M. Ringold, and M. Danielsen.** 1987. Lipofection: a highly efficient, lipid mediated DNA-transfection procedure. Proc. Natl. Acad. Sci. USA **84**:7413–7417.
15. **Fuerst, T. R., P. L. Earl, and B. Moss.** 1987. Use of a hybrid vaccinia virus-T7 RNA polymerase system for expression of target genes. Mol. Cell. Biol. **7**:2538–2544.
16. **Gething, M. J., K. McCammon, and J. Sambrook.** 1986. Expression of wild type and mutant forms of influenza hemagglutinin: the role of folding in intracellular transport. Cell **46**:939–950.
17. **Goldstein, J. L., M. S. Brown, R. G. W. Anderson, D. W. Russell, and W. J. Schneider.** 1985. Receptor-mediated endocytosis: concepts emerging from the LDL receptor system. Annu. Rev. Cell Biol. **1**:1–39.
18. **Hannink, M., and D. J. Donoghue.** 1986. Cell surface expression of membrane-anchored v-sis gene products: glycosylation is not required for cell surface transport. J. Cell Biol. **103**:2311–2322.
19. **Hiebert, S. W., and R. A. Lamb.** 1988. Cell surface expression of glycosylated, nonglycosylated, and truncated forms of a cytoplasmic protein pyruvate kinase. J. Cell Biol. **107**:865–876.
20. **Hiti, A. L., and D. P. Nayak.** 1982. Complete nucleotide sequence of the neuraminidase gene of human influenza virus A/WSN/33. J. Virol. **41**:730–734.
21. **Hurtley, S. M., and A. Helenius.** 1989. Protein oligomerization in the endoplasmic reticulum. Annu. Rev. Cell Biol. **5**:277–307.
22. **Iacopetta, B. J., S. Rothenberger, and L. C. Kuhn.** 1988. A role for the cytoplasmic domain in transferrin receptor sorting and coated pit formation during endocytosis. Cell **54**:485–489.
23. **Jabbar, M. A., and D. P. Nayak.** 1987. Signal processing, glycosylation, and secretion of mutant hemagglutinins of a human influenza virus by *Saccharomyces cerevisiae*. Mol. Cell. Biol. **7**:1476–1485.
24. **Jabbar, M. A., and D. P. Nayak.** 1990. Intracellular interaction of human immunodeficiency virus type I (ARV-2) envelope glycoprotein gp160 with CD4 blocks the movement and maturation of CD4 to the plasma membrane. J. Virol. **64**:6297–6304.
25. **Jing, S., T. Spencer, K. Miller, C. Hopkins, and I. S. Trowbridge.** 1990. Role of the human transferrin receptor cytoplasmic domain in endocytosis: localization of a specific signal sequence for internalization. J. Cell Biol. **110**:283–294.
26. **Kornfeld, R., and S. Kornfeld.** 1985. Assembly of asparagine-linked oligosaccharides. Annu. Rev. Biochem. **54**:631–664.
27. **Kornfeld, S., and I. Mellman.** 1989. The biogenesis of lysosomes. Annu. Rev. Cell Biol. **5**:483–525.
28. **Ktistakis, N. T., D. Thomas, and M. G. Roth.** 1990. Characteristics of the tyrosine recognition signal for internalization of transmembrane surface glycoproteins. J. Cell Biol. **111**:1393–1407.
29. **Kuhn, L. C., A. McClelland, and F. H. Ruddle.** 1984. Gene transfer, expression, and molecular cloning of the human tranferrin receptor gene. Cell **37**:95–103.
30. **Laemmli, U. K.** 1970. Cleavage of structural proteins during the assembly of the head of bacteriophage T4. Nature (London) **227**:680–685.
31. **Lazarovits, J., and M. Roth.** 1988. A single amino acid change in the cytoplasmic domain allows the influenza virus hemagglutinin to be endocytosed through coated pits. Cell **53**:743–752.
32. **Le Bivic, A., F. X. Real, and E. Rodriguez-Boulan.** 1989. Vectorial targeting of apical and basolateral plasma membrane proteins in a human adenocarcinoma epithelial cell line. Proc. Natl. Acad. Sci. USA **86**:9313–9317.
33. **Lehrman, M. A., J. L. Goldstein, M. S. Brown, D. W. Russel, and W. J. Schneider.** 1988. Internalization-defective LDL receptors produced by genes with nonsense and frameshift mutations that truncate the cytoplasmic domain. Cell **41**:735–743.
34. **Lobigs, M., Z. Hongxing, and H. Garoff.** 1990. Function of Semliki Forest virus E3 peptide in virus assembly: replacement of E3 with an artificial signal peptide abolishes spike heterodimerization and surface expression of E1. J. Virol. **64**:4346–4355.
35. **Mackett, M., G. L. Smith, and B. Moss.** 1985. The construction and characterization of vaccinia virus recombinants expressing foreign genes, p. 191–211. *In* D. Rickwood and B. D. Hames (ed.), DNA cloning, vol. 2. IRL Press, Washington, D.C.
36. **Martin, R. G., and B. N. Ames.** 1961. A method for determining the sedimentation behavior of enzymes: application to protein mixtures. J. Biol. Chem. **236**:1372–1379.
37. **McQueen, N. L., D. P. Nayak, L. V. Jones, and R. W. Compans.** 1984. Chimeric influenza virus hemagglutinin containing either the NH_2 terminus or the COOH terminus of G protein of vesicular stomatitis virus is defective in transport to the cell surface. Proc. Natl. Acad. Sci. USA **81**:395–399.
38. **McQueen, N. L., D. P. Nayak, E. B. Stephens, and R. W. Compans.** 1986. Polarized expression of a chimeric protein in which the transmembrane and cytoplasmic domains of the influenza virus hemagglutinin have been replaced by those of the vesicular stomatitis virus G protein. Proc. Natl. Acad. Sci. USA **83**:9318–9322.
39. **McQueen, N. L., D. P. Nayak, E. B. Stephens, and R. W. Compans.** 1987. Basolateral expression of a chimeric protein in which the transmembrane and cytoplasmic domains of vesicular stomatitis virus G protein have been replaced by those of the influenza virus hemagglutinin. J. Biol. Chem. **262**:16233–16240.
40. **Nath, S. T., and D. P. Nayak.** 1990. Function of two discrete regions is required for nuclear localization of polymerase basic protein 1 of A/WSN/33 influenza virus (H1 N1). Mol. Cell. Biol. **10**:4139–4145.
41. **Nayak, D. P., and M. A. Jabbar.** 1989. Structural domains and organizational conformation involved in the sorting and transport of influenza virus transmembrane proteins. Annu. Rev. Microbiol. **43**:465–501.
42. **Ng, D. T. W., R. E. Randall, and R. A. Lamb.** 1989. Intracellular maturation and transport of the SV5 type II glycoprotein hemagglutinin-neuraminidase: specific and transient association with GRP78-BiP in the endoplasmic reticulum and extensive internalization from the cell surface. J. Cell Biol. **109**:3273–3289.
43. **Omary, M. B., and I. S. Trowbridge.** 1981. Biosynthesis of the human transferrin receptor in cultured cells. J. Biol. Chem. **256**:4715–4718.
44. **Palese, P., K. Tobita, M. Ueda, and R. W. Compans.** 1974. Characterization of temperature sensitive influenza virus mutants defective in neuraminidase. Virology **61**:397–410.
45. **Paterson, R. G., and R. A. Lamb.** 1990. Conversion of a class II integral membrane protein into a soluble and efficiently secreted protein: multiple intracellular and extracellular oligomeric and

conformational forms. J. Cell Biol. **110**:999–1011.

46. **Peters, C., M. Braun, B. Weber, M. Wendland, B. Schmidt, R. Pohlmann, A. Waheed, and K. von Figura.** 1990. Targeting of a lysosomal membrane protein: a tyrosine-containing endocytosis signal in the cytoplasmic tail of lysosomal acid phosphatase is necessary and sufficient for targeting to lysosomes. EMBO J. **9**:3497–3506.
47. **Pfeffer, S. R., and J. E. Rothman.** 1987. Biosynthetic protein transport and sorting by the endoplasmic reticulum and Golgi. Annu. Rev. Biochem. **56**:829–852.
48. **Puddington, L., C. E. Machamer, and J. K. Rose.** 1986. Cytoplasmic domains of cellular and viral integral membrane proteins substitute for the cytoplasmic domain of the vesicular stomatitis virus glycoprotein in transport to the plasma membrane. J. Cell Biol. **102**:2147–2157.
49. **Rademacher, T. W., R. B. Parekh, and R. A. Dwek.** 1988. Glycobiology. Annu. Rev. Biochem. **57**:785–838.
50. **Roth, M. G., C. Doyle, J. Sambrook, and M. J. Gething.** 1986. Heterologous transmembrane and cytoplasmic domains direct functional chimeric influenza virus hemagglutinins into the endocytic pathway. J. Cell Biol. **102**:1271–1283.
51. **Sargiacomo, M., M. Lisanti, L. Graeve, A. Le Vivic, and E. Rodriguez-Boulan.** 1989. Integral and peripheral protein composition of the apical and basolateral membrane domains in MDCK cells. J. Membr. Biol. **107**:277–286.
52. **Schneider, C., R. Sutherland, R. Newman, and M. Greaves.** 1982. Structural features of the cell surface receptor for transferrin that is recognized by the monoclonal antibody OKT9. J. Biol. Chem. **257**:8516–8522.
53. **Sivasubramanian, N., and D. P. Nayak.** 1987. Mutational analysis of the signal-anchor domain of influenza virus neuraminidase. Proc. Natl. Acad. Sci. USA **84**:1–5.
54. **Verghese, J. N., W. G. Laver, and P. M. Colman.** 1983. Structure of the influenza virus glycoprotein antigen neuraminidase at 2.9 A resolution. Nature (London) **289**:366–378.
55. **Williams, M. A., and M. Fukuda.** 1990. Accumulation of membrane glycoproteins in lysosomes requires a tyrosine residue at a particular position in the cytoplasmic tail. J. Cell Biol. **111**:955–966.
56. **Wilson, I., J. Skehel, and D. Wiley.** 1981. Structure of hemagglutinin membrane glycoprotein of influenza virus at 3 A resolution. Nature (London) **289**:366–373.
57. **Yewdell, J. W., A. Yellen, and T. Bachi.** 1988. Monoclonal antibodies localize events in the folding, assembly and intracellular transport of influenza virus hemagglutinin glycoprotein. Cell **52**:843–852.